IMAGING MAGNETIC SUSCEPTIBILITY OF THE HUMAN KNEE JOINT AT 3 AND 7 TESLA

Hongjiang Wei[1], Bin Wang[1], Xiaopeng Zong[2], Weili Lin[2], Nian Wang[1], and Chunlei Liu[1,3]

[1]*Brain Imaging and Analysis Center, Duke University, Durham, NC, United States,* [2]*Biomedical Research Imaging Center, University of North Carolina at Chapel Hill, NC, United States,* [3]*Depatment of Radoilogy, School of Medicine, Duke University, NC, United States*

Purpose: The knee joint is one of the most important joints in the human body with several intricate structures and complex interfaces including bones, tendons, muscles, fat, ligaments, cartilages and meniscuses. Each of these components has unique molecular and cellular composition and microstructures and thus may exhibit varying magnetic susceptibility. Quantitative susceptibility mapping (QSM) has been widely investigated in the brain, e.g. for quantifying iron deposits and myelination [1-3]. However, these techniques have not been successfully implemented in the knee. Application of QSM in the knee is faced with an additional technical challenge which is not problematic for QSM in the brain - the presence of fat in the knee. A couple of recent studies have combined water-fat separation with QSM [4, 5]. The purpose of this work was to develop and demonstrate feasibility of water-fat separated QSM in the knee as well as to evaluate the susceptibility properties of different anatomical structures within the knee joint. Imaging susceptibility of the knee may aid in assessing knee joint diseases and disorders.

Methods: Healthy volunteers were scanned on 3T (GE Healthcare, Waukesha, WI) and 7T (Siemens Healthcare, Erlangen, Germany) MRI scanners where the 7T scanner is housed in the Biomedical Research Imaging Center, UNC-Chapel Hill. At 3T, a birdcage head coil was used for the 3D knee acquisitions. The acquisition parameters of the GRE sequence were: TR=50ms, TE_1=3ms, ΔTE=1.64ms, 16 echoes, and flip angle=10°, matrix size=136×192×108, voxel size=1.3×1.3×1.3mm^3. At 7T, a dedicated 28-channel knee coil was used. A sagittal 3D fast low-angle shot (FLASH) sequence was used. The scan parameters were: TR=35ms, TEs=[1.61, 1.96, 2.31, 2.89, 3.24, 3.58]ms, flip angle=10°, matrix size=380×384×88, voxel size=0.4×0.4×1.6mm^3. Fat is present within the knee in the forms of adipose tissue. The presence of fat introduces significant chemical shift which confounds the estimate of the B0 field map. Fat is composed of multiple spectral peaks, each of which processes at a different frequency than water. The presence of these fat peaks must be included in the reconstruction to ensure accurate estimation of the B0 field map. The B0 field map is estimated using a chemical shift encoded reconstruction [6] by the cost function in a L2-norm minimization procedure.

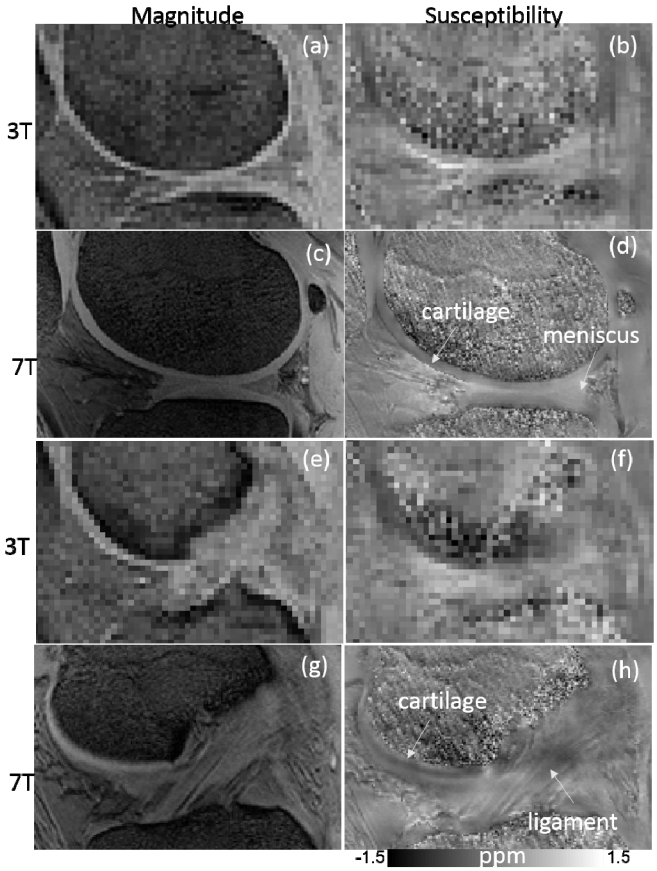

Fig. 1. Magnitude and corresponding susceptibility at 3T and 7T. Arrows indicate cartilages, meniscus and ligaments.

$$\min_{\rho_w,\rho_f,f_B}\left\{\sum_{n=1}^{N}\left\|s(t_n)-e^{-i2\pi f_B t_n}\left(\rho_w+\rho_f\sum_{j=1}^{M}\alpha_j e^{-i2\pi\Delta f_j t_n}\right)\right\|_2\right\} \quad (1)$$

where N is the number of echoes and M (M=6) is number of the spectral peaks of the fat. The chemical shifts Δf_i for each peak are known a priori. The relative amplitudes of the fat peaks α_i with $\Sigma\alpha_i$=1 are also predefined. After the B0 filed map is estimated, the susceptibility map can be obtained by solving the following equation:

$$\min_{\chi}\left\{\left\|W_{\text{Image}}\left(F^{-1}D_2\cdot F\chi-\varphi\right)\right\|_2+TV(\chi)\right\} \quad (2)$$

F and F^{-1} are Fourier transform and inverse Fourier transform, respectively. The weighting function W_{image} were estimated from the unwrapped phase with thresholding. The threshold parameters could be [90%-99% percentile] of the phase values for the knee data. The weights were the inverse of the thresholded phase values. *TV* stands for the total variation term.

RESULTS: Fig.1 compares the magnitude images and the corresponding susceptibility maps at 3T and 7T. The magnetic susceptibility maps at 3T (b) and 7T (d) both clearly delineate the knee joint structures. The cartilage and meniscus, as indicated by the arrows in Fig. 1(d), can be easily distinguished from each other due to the different susceptibility properties. Generally, miniscus appears more paramagnetic than cartilage. With improved resolution at 7T, susceptibility maps reveal excellent image quality with fine delineation of the details of cartilage and meniscus among other structures. For example, cartilage and ligament can be distinguished in QSM (Fig. 1(h)). Interestingly, the femur articular cartilage appears to have three parallel layers as indicated by the arrow in Fig. 1(h), which can not be clearly seen from the magnitude in Fig. 1(g). The susceptibility maps without and with fat separation at 7T are compared. QSM with fat supression exhibits different susceptibilty properties of structures (subcutaneous, vein, etc.) as indicated by the arrows in Fig. 2(b), which can not be seen from the susceptibility map without fat supression in Fig. 2(a).

CONCLUSION: QSM technique was applied for knee joint with water-fat separation. QSM resulted in very similar susceptibility properties both in 3T and 7T, while the QSM results in this study show the superiority of 7T MRI compared to 3T partially due to the higher signal to noise ratio and higher spatial resolution. Moreover, QSM provides a quantitative contrast that reflects spatial variation in tissue composition. The cartilage and ligament were darker than surrounding tissue due to the diamagnetic properties while the meniscus shows paramagnetic property. The different susceptibility properties may relate to the local microsturture orientaions with respect to B0 field. This method provides a quantitative tools for characterizing different type of tissues in the knee which may be useful for the evaluation of various knee diseases.

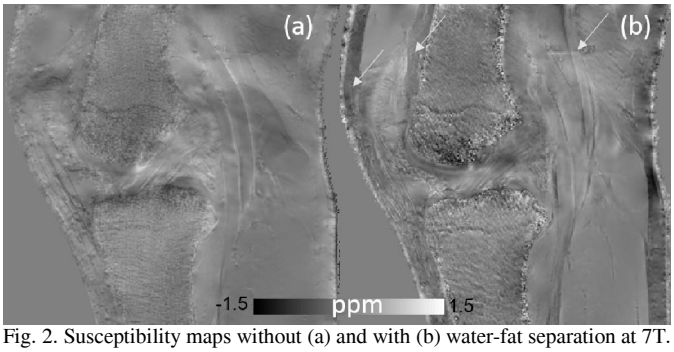

Fig. 2. Susceptibility maps without (a) and with (b) water-fat separation at 7T.

REFERENCES: 1. Li W et al, *NMR in Biomedicine.* 2014,27; 219-227. 2. Deistung A et al, PLoS One, 2013, Epub. 3. Cao W et al, Neuroimage, 2014 Epub. 4.Dimov A et al. MRM. 2014, Epub. 5. Sharma S et al. MRM. 2014, Epub. 6.Yu H et al. MRM. 2005, 54; 1032-1039.